

Projected index computed tomography

Adam M. Zysk, J. Josh Reynolds, Daniel L. Marks, and P. Scott Carney

*Department of Electrical and Computer Engineering, Beckman Institute for Advanced Science and Technology,
University of Illinois at Urbana—Champaign, Urbana, Illinois 61801*

Stephen A. Boppart

*Department of Electrical and Computer Engineering, Bioengineering Program, Beckman Institute for Advanced Science and Technology,
College of Medicine, University of Illinois at Urbana—Champaign, 405 North Mathews Avenue, Urbana, Illinois 61801*

Received November 13, 2002

Projected index computed tomography (PICT) is a new imaging technique that provides a computed reconstruction of the index of refraction of a sample. PICT makes use of data from standard optical coherence tomography images taken from several view angles to determine a mapping of the refractive indices of the sample. A rectilinear propagation model is assumed, so the data are understood to be related to the line integral of the refractive index in the beam paths. These data thus provide a set of angular projections of the sample. The spatial distribution of the index of the object may then be reconstructed by use of standard filtered backprojection techniques. The resultant PICT images are free of the spatial distortion that is inherent in standard optical cross-sectional images and correspond well to the manufactured dimensions of specific samples. © 2003 Optical Society of America

OCIS codes: 110.4500, 110.6960, 120.5710, 170.3010, 290.3030.

Optical coherence tomography (OCT) and confocal scanning laser microscopy (CSLM) are well-known optical methods of nondestructive subsurface imaging.^{1,2} OCT systems make use of near-infrared light to probe samples by use of interferometric range-finding techniques that result in maps of the effective (distorted) position of scattering inclusions in the sample. CSLM forms an image by scanning the focus of laser light into the sample and blocking out-of-focus reflections with a pinhole, thereby detecting the response at the focus.

OCT and CSLM images suffer from distortions^{3,4} caused by inhomogeneities of the refractive index. A typical OCT system measures the optical path length to scattering objects embedded in the sample by means of an interferometric range-finding technique. The optical path length of the light through the sample is determined by the index of refraction of the sample along the beam path. Because the index of refraction of most samples is not constant, a depth-dependent distortion of the imaged object structure is evident.

Recently the tools of computed tomography were applied to optical microscopy with promising results.⁵ For example, optical projection tomography⁶ provides three-dimensional imaging by computing tomographs of the uncorrelated source density from data consisting of optical images of the sample from many view angles. This technique is capable of imaging biological samples thicker than those that can be imaged with OCT or confocal microscopy while it reduces distortion. Here we present an optical technique for distortion-corrected index-of-refraction imaging. Computational reconstruction of the sample is generated from a data set consisting of a series of OCT images taken at incremental angles of projection. We refer to this method as projected index computed tomography (PICT).

The distortion in an OCT image is evident when a known reflective surface is placed below a sample for reference. The imaged position of the reflective surface is determined by the total optical path delay,

which is a result of the medium's inhomogeneous refractive index. Here the word "index" refers to the group index at the center wavelength of the laser. The image of the reflective surface becomes displaced in depth by the aggregate refractive index of the sample located above it. Previous investigations showed that quantifying this displacement makes OCT an effective method for determining the index of refraction for certain biological materials.⁷ Because, to first order, the displacement of each point on the reflective surface is due to the total integrated index along the ray path of the material located directly above it, the displacement of the reflector in such an image represents the projection of the index of refraction of the sample, i.e., the Radon transform of the index of refraction of the object.

For generation of a computed reconstruction, the PICT data must consist of displaced-reflector images taken at multiple angles. The data are analogous to those of medical computed tomography imaging in which x-ray beam attenuation that is due to the patient is determined by use of a rotating set of sources and sensors. In computed tomography the projection data may then be processed to yield the absorption index at each point within the sample area. One obtains the reconstruction of the object structure by performing a filtered summation of the angular projection data for each point: This is a technique called filtered backprojection (an implementation of the inverse Radon transform). A general form of the filtered backprojection operation can be written as

$$f(x, y) = \int_0^\pi p^f(x \cos \phi + y \sin \phi, \phi) d\phi, \quad (1)$$

where

$$p^f(r, \phi) = \int_{-\infty}^{\infty} |\omega| P(\omega, \phi) \exp(2\pi j\omega r) d\omega \quad (2)$$

is filtered projection data. $f(x, y)$ is the reconstructed data, x and y are rectangular coordinates, ϕ is the

angle from the y axis, r is the radial distance from the origin, ω is the spatial frequency, and $P(\omega, \phi)$ is the Fourier domain representation of the projection data.^{8,9}

Beam paths traversing a refractive-index boundary are governed by Snell's law, which describes the angle of refraction in terms of the angle of incidence and the indices of the materials. The indices of refraction within biological tissue typically vary by 10% or less about an average index of approximately $n = 1.4$. In the current PICT implementation it is therefore reasonable to assume that the index variation is small enough that one may ignore perturbations of the beam path, with the exception of a small number of easily identifiable extreme points. To first-order perturbation in the refractive index, ray paths do not change.¹⁰ The same assumption can also be made for other materials with small index perturbations.

Each displaced-reflector image was taken with the system shown in Fig. 1. The system employs a frequency-doubled Nd:YVO₄-pumped titanium:sapphire (Ti:Saph) source centered at $\lambda = 800$ nm, which, after fiber coupling into ultrahigh-numerical-aperture fiber, allows for approximately 80 nm of bandwidth.¹¹ Approximately 10 mW of power is incident upon the sample from a 50/50 fiber splitter that also couples light reflected from a galvanometer-based delay line. The sample is both rotated and translated by a pair of computer-controlled stages, which allow for precise movement of the sample. The system produces standard OCT images with a resolution of approximately $3.5 \mu\text{m}$.

The resolution of a PICT image depends on both the number of projections and the resolution of each displaced-reflector OCT image. Fundamental concepts of computed tomography indicate that the theoretical resolution limit of a reconstructed image is equivalent to or better than the resolution of the projections themselves, provided that an adequate number of projections exists.¹² Therefore a PICT image resulting from a filtered backprojection reconstruction will have a resolution near that of a standard OCT image (approximately $1\text{--}10 \mu\text{m}$). Because of the nonuniform coverage of projections, tomographically reconstructed images have a spatially varying resolution. Pixels near the center of the image are sampled at a higher rate than those at the edges, where interpolation routines are relied on more heavily. This leads to higher resolution near the center of the image.

Using our OCT system, we acquired displaced-reflector images of an optical cement-filled capillary tube. One displaced-reflector image is shown in Fig. 2A. Each displaced-reflector image was processed by use of a surface detection routine designed to find the location of the weighted maximum pixel in each column. In the event that no strong reflection was detected in a given column (i.e., the assumption of small index variation was invalid), as is evident near the edges of the projection data for a radially symmetric sample, data were linearly interpolated from nearby available samples. The distance to the reflector with no sample present was then subtracted from the distance measurement in each projection data set. Each set of projection data was also cen-

tered to compensate for wobble in the sample support shaft. Figure 2B shows the projection data from one displaced-reflector image after this processing.

The final image was constructed by use of the *iradon* Matlab routine, which implements a filtered

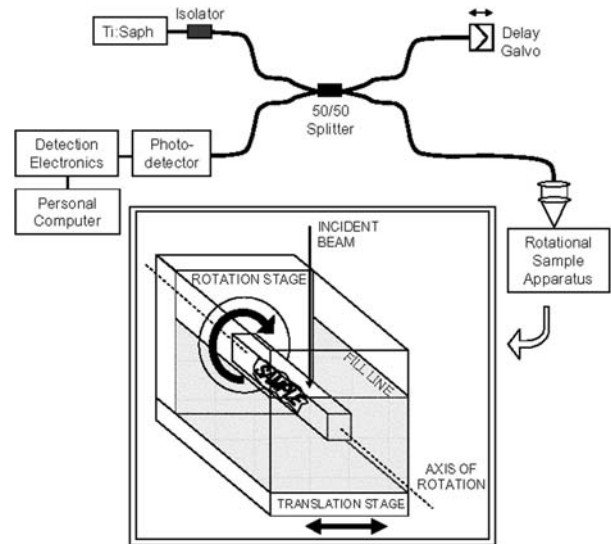


Fig. 1. Schematic of the PICT setup. The computer-controlled rotational stage allows for the acquisition of incremental angularly displaced projection images.

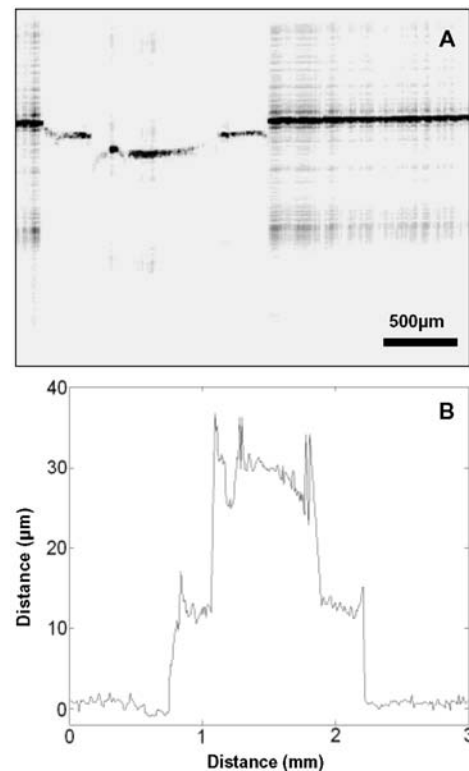


Fig. 2. PICT projection data. A, Single displaced-reflector OCT image of a filled capillary tube. Displacements in the reflector in the vertical direction represent the projected index along the beam paths. B, Corresponding projection data after the displaced-reflector image is processed. Processing includes reflector detection, surface subtraction, low reflection interpolation, and centering.

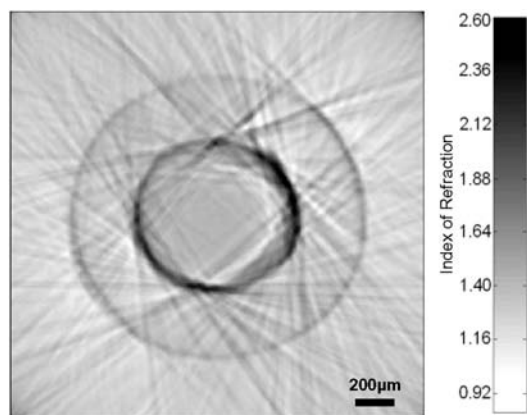


Fig. 3. Cross-sectional PICT image of a capillary tube. The tube is filled with optical cement and placed in index-matching fluid for imaging. A PICT image represents the spatial map of the indices of the sample. Linear artifacts are the result of sharp discontinuities in projected data. Equally commonly in computed tomography, these artifacts can be removed with more-advanced computed tomography algorithms. The gray scale indicates the related index values.

backprojection algorithm. A Hamming windowed Ram-Lak filter and a linear interpolator were also implemented to improve noise rejection and to complete the image data between projection angles. It should be noted that a reconstruction was also performed without the previously mentioned centering step, which yielded a spatially offset image equivalent to that presented here.

Figure 3 shows a reconstructed PICT image of a capillary tube composed of 160 angular projections at 1.5° increments. The glass capillary tube ($n \approx 1.47$) was filled with optical cement ($n \approx 1.56$) and submerged in an index-matching fluid (ethylene glycol, $n \approx 1.43$) to facilitate the beam path approximations mentioned above. The straight-line artifacts that are present in Fig. 3 are typical of computed tomography images. Note that the PICT image does not suffer from the spatial distortion of a standard OCT or CSLM image. In fact, the distortions that are commonly present in a standard OCT image are used in the formation of the PICT index-mapping image.

The images were acquired with an acromat lens ($f = 40$ mm) with a calculated confocal parameter of 1.35 mm. This configuration yields an approximately collimated beam over the sample region. The data acquisition was performed in approximately 1.5 h because of the slow acquisition rate of the OCT system and the large quantity of images. Acquisition time potentially can be reduced to approximately 1 min by incorporation of a rapid-scanning optical delay in the reference arm. The data processing time was approximately 15 min on a personal computer with a 1.8-GHz Pentium 4 processor and could be shortened with improved algorithms or parallel computation.

The PICT image corresponds well to the manufacturer dimensions of the capillary tube (inner diameter, 0.86 ± 0.04 mm; outer diameter, 1.5 ± 0.04 mm).

Measured dimensions in the PICT image are within 3% of these dimensions. Sensitivity to index changes within a PICT image lies within the range necessary for biological imaging. Analysis of glass capillary tubes filled with optical cements of various indices showed that index variations as small as $\Delta n = 0.02$ can be detected. We measured the manufacturer-specified index of each cement at ~ 800 nm by determining the path displacement in an OCT image of the cement on a glass slide.⁷

In this Letter we have demonstrated a new technique called projected index computed tomography (PICT) for generating image-based maps of the indices of refraction of materials. Future investigations will focus on new algorithms to improve resolution based on a modified reconstruction algorithm that accounts for beam path perturbations. This technique will account for solutions to the eikonal equation that describes the beam path through a medium of known refractive-index values¹³ beyond the first-order linear approximation implicit here. Iterative recalculation of index values from improved beam path approximations will lead to the enhancement of the reconstruction algorithms used here. Research for the future will include investigation of biological and material applications for this technique.

This research was supported by the National Science Foundation (grant BES-0086696), the Whitaker Foundation, and the Beckman Institute. S. A. Boppart's e-mail address is boppart@uiuc.edu.

References

1. D. Huang, E. A. Swanson, C. P. Lin, J. S. Schuman, W. G. Stinson, W. Chang, M. R. Hee, T. Flotte, K. Gregory, C. A. Puliafito, and J. G. Fujimoto, *Science* **254**, 1178 (1991).
2. S. E. Ilyin, M. C. Flynn, and C. R. Plata-Salamán, *J. Neurosci. Meth.* **108**, 91 (2001).
3. V. Westphal, A. M. Rollins, S. Radhakrishnan, and J. A. Izatt, *Opt. Express* **10**, 397–404 (2002), <http://www.opticsexpress.org>.
4. A. Diaspro, F. Federici, and M. Robello, *Appl. Opt.* **41**, 685 (2002).
5. D. L. Marks, R. A. Stack, D. J. Brady, D. C. Munson, and R. B. Brady, *Science* **284**, 2164 (1999).
6. J. Sharpe, U. Ahlgren, P. Perry, B. Hill, A. Ross, J. Hecksher-Sørensen, R. Baldock, and D. Davidson, *Science* **296**, 541 (2002).
7. G. J. Tearney, M. E. Brezinski, J. F. Southern, B. E. Bourma, M. R. Hee, and J. G. Fujimoto, *Opt. Lett.* **20**, 2258 (1995).
8. F. Natterer and F. Wübbeling, *Mathematical Methods in Image Reconstruction* (Society for Industrial and Applied Mathematics, Philadelphia, Pa., 2001).
9. R. A. Brooks and G. DiChiro, *Phys. Med. Biol.* **21**, 689 (1976).
10. C. M. Vest, *Appl. Opt.* **24**, 4089 (1985).
11. D. L. Marks, A. L. Oldenburg, J. J. Reynolds, and S. A. Boppart, *Opt. Lett.* **27**, 2010 (2002).
12. A. Caponnetto and M. Bertero, *Inverse Probl.* **13**, 1191 (1997).
13. M. Born and E. Wolf, *Principles of Optics* (Pergamon, Oxford, 1964).